Supplemental material

Spindle checkpoint-independent inhibition of mitotic chromosome segregation by Drosophila Mps1

Friederike Althoff*, Roger E. Karess†, Christian F. Lehner*

* Institute of Molecular Life Sciences, University of Zurich, Winterthurerstrasse 190, 8057 Zurich, Switzerland
† CNRS, Institut Jacques Monod, UMR7592, Université Paris Diderot, Paris Cedex 13, France.

The Supplemental Material includes:

Supplemental material and methods

Plasmid constructs

pCaSpeR4-EGFP-Mps^{kd}

Construct for expression of kinase-dead Mps1 N-terminally tagged with EGFP under control of the cis-regulatory region of *Mps1*. *pCaSpeR-EGFP-Mps1* (Fischer *et al.*, 2004) was cut with NotI and Asp718. The resulting *EGFP-Mps1* fragment was transposed into the corresponding sites of *pBluescriptIIKS(-)* resulting in cloning intermediate 1 (*pBluescript-EGFP-Mps1*). The point mutation A1778C in the *Mps1* coding sequence leading to the amino acid exchange Asp478 to Ala (D478A) was introduced into cloning intermediate 1 using the QuikChangeII site-directed mutagenesis kit (Stratagene) and the primers AF5 (GTTGATCG***C***TTTTGGCATAGCCAG) and AF6 (GCTATGCCAAAA***G***CGATCAACTTC). The resulting cloning intermediate 2 (*pBluescript-EGFP-Mps1^{kd}*) and *pCaSpeR-EGFP-Mps1* were digested with BglII, followed by replacement of the relevant BglII fragment in *pCaSpeR-EGFP-Mps1* in order to arrive at *pCaSpeR-EGFP-Mps1^{kd}*.

pCaSpeR4-EGFP-Mps1^{N}

Construct for expression of the N-terminal domain of Mps1 (aa 1–332) N-terminally tagged with EGFP under control of the cis-regulatory region of *Mps1*. Inverse PCR was performed with cloning intermediate 1 as template using the primers AF1 (ATT***CTCGAG***TTTTAAAATATTAGATGTCTTGTG) and AF2 (AAC***CTCGAG*****TAA**GCACGAAAGCTCAGCTA), which introduced an XhoI site instead of the sequence of *Mps1^{C}*. Cutting of the product with XhoI and ligating resulted in cloning intermediate 3 (*pBluescript-EGFP-Mps1^{N}*). Cloning intermediate 3 was digested with NotI and Asp718, and the excised fragment containing the *EGFP-Mps1^{N}* sequence was transposed into the corresponding sites in *pCaSpeR4* resulting in *pCaSpeR4-EGFP-Mps1^{N}*.

pCaSpeR4-EGFP-Mps1^{C}

Construct for expression of the C-terminal domain of Mps1 (aa 325–630) N-terminally tagged with EGFP under control of the cis-regulatory region of *Mps1*. Inverse PCR was performed with cloning intermediate 1 as template using the primers AF3

(TCCC***CCATGG***CATCTAATATTTTAAAAATCAAGAA) and AF4 (CGGGGCACAGGCGTGG), which introduced an NcoI site instead of the sequence of *Mps1*^{N}. Cutting of the product with NcoI and ligating resulted in cloning intermediate 4 (*pBluescript-EGFP-Mps1*^{C}). Cloning intermediate 4 was digested with NotI and Asp718, and the excised fragment containing the *EGFP-Mps1*^{C} sequence was transposed into the corresponding sites in *pCaSpeR4* resulting in *pCaSpeR4-EGFP-Mps1*^{C}.

pUAST-EGFP-Mps1 and *pUAST-EGFP-Mps1*^{kd}
Constructs for ectopic expression of wild type or kinase dead Mps1 N-terminally tagged with EGFP by the UAS/GAL4 system. *EGFP* was amplified from *pUAST-EGFP-Cenp-C(C)* (Heeger *et al.*, 2005) using the primers AF9 (GGGAATTGGGAATTCGTTAAC) and AF10 (GGATTTCTG***GCGGCCGC***CTTGTACAGCTCGTCCATG), which introduced a flanking NotI site. After digestion with BglII and NotI, the PCR fragment was transposed into the corresponding sites in *pUAST* resulting in cloning intermediate 5 (*pUAST-EGFPΔTAA)*. The *Mps1* and *Mps1*^{kd} sequences were amplified from *pCaSpeR4-EGFP-Mps1* or *pCaSpeR4-EGFP-Mps1*^{kd} using the primers AF12 (GAATAAATCG***GCGGCCGC***GATGACCACGCCTGTGCC) and AF13 (TT***GGTACC***TTAATTGCTGTTGGCGGTTC), which introduced flanking NotI or Asp718 sites, respectively. After digestion with NotI and Asp718, the PCR fragments were transposed into the corresponding sites in cloning intermediate 5 resulting in *pUAST-EGFP-Mps1* and *pUAST-EGFP-Mps1*^{kd}.

pUAST-EGFP-Mps1^{N}
Construct for ectopic expression of the N-terminal domain of Mps1 (aa 1–332) N-terminally tagged with EGFP by the UAS/GAL4 system. The *Mps1*^{N} sequence was amplified from the EST plasmid *LD04521* (Rubin *et al.*, 2000) using the primers AF12 (GAATAAATCG***GCGGCCGC***GATGACCACGCCTGTGCC) and AF39 (GTATA***GGTACC***TTACTTGATTTTTAAAATATTAGATGTC), which introduced a flanking NotI or Asp718 site, respectively. After digestion with NotI and Asp718, the PCR fragment was transposed into the corresponding sites in *pUAST-EGFP-MCS* (Schittenhelm *et al.*, 2007) resulting in *pUAST-EGFP-Mps1*^{N}.

pUAST-EGFP-Mps1^{C}
Construct for ectopic expression of the C-terminal domain of Mps1 (aa 325–630) N-terminally tagged with EGFP by the UAS/GAL4 system. The *Mps1*^{C} sequence was amplified from the EST plasmid *LD04521* (Rubin *et al.*, 2000) using the primers AF13 (TT***GGTACC***TTAATTGCTGTTGGCGGTTC) and AF40 (CTCCAGAGCAG***GCGGCCGC***CAAGACATCTAATATTTTAAAAATC), which introduced a flanking NotI or Asp718 site, respectively. After digestion with NotI and Asp718, the PCR fragment was transposed into the corresponding sites in *pUAST-EGFP-MCS* (Schittenhelm *et al.*, 2007) resulting in *pUAST-EGFP-Mps1*^{C}.

pUAST-EGFP-Mps1^{Ckd}
Construct for ectopic expression of the kinase dead C-terminal domain of Mps1 (aa 325–630) N-terminally tagged with EGFP by the UAS/GAL4 system. The point mutation A1778C was introduced into the EST plasmid *LD04521* (Rubin *et al.*, 2000) using the QuikChangeII site-directed mutagenesis kit (Stratagene) and the primers AF5 (GTTGATCG***C***TTTTGGCATAGCCAG) and AF6 (GCTATGCCAAAA***G***CGATCAACTTC). This step resulted in cloning intermediate 6 (*LD04521-Mps1*^{kd}). The *Mps1*^{Ckd} sequence was amplified from cloning intermediate 6 using the primers AF13 (TT***GGTACC***TTAATTGCTGTTGGCGGTTC) and AF40 (CTCCAGAGCAG***GCGGCCGC***CAAGACATCTAATATTTTAAAAATC), which introduced a flanking NotI or Asp718 site, respectively. After digestion with NotI and Asp718, the PCR fragment

was transposed into the corresponding sites in *pUAST-EGFP-MCS* (Schittenhelm *et al.*, 2007) resulting in *pUAST-EGFP-Mps1*^{Ckd}.

pUAST-EGFP-bub1
Construct for ectopic expression of Bub1 N-terminally tagged with EGFP by the UAS/GAL4 system. The *bub1* sequence was amplified from the EST plasmid *LD22858* (Rubin *et al.*, 2000) using the primers CS6 (CGCGTC***GGTACC***AGATGGCCATGCACTCGTA) and CS7 (GAATA***TCTAGA***TTATCGTCGATGCAGGATGT), which introduced a flanking Asp718 or XbaI site, respectively. After digestion with Asp718 and XbaI, the PCR fragment was transposed into the corresponding sites in *pUAST-EGFP-MCS* (Schittenhelm *et al.*, 2007) resulting in *pUAST-EGFP-bub1*.

pUAST-EGFP-mad2
Construct for ectopic expression of Mad2 N-terminally tagged with EGFP by the UAS/GAL4 system. The *mad2* sequence was amplified from genomic *Drosophila melanogaster* DNA using the primers RaS232 (CGACT***GCGGCCGC***AATGTCAACTGCCCAGGCG) and RaS233 (GGTAC***GGTACC***TTAAGTGCTCATCTTGTAGTTG), which introduced a flanking NotI or Acc65I site, respectively. After digestion with NotI and Acc65I, the PCR fragment was transposed into the corresponding sites in *pUAST-EGFP-MCS* (Schittenhelm *et al.*, 2007) resulting in *pUAST-EGFP-mad2*.

pUAST-EGFP-STOP
Constructs for ectopic expression of EGFP by the UAS/GAL4 system. These plasmids were designed to serve as control plasmids for the expression effects of EGFP-BubR1. The point mutation A3611G in the *bubR1* coding sequence leading to the amino acid exchange Lys1204 to Arg (K1204R) was introduced into the EST plasmid *LD23835* (Stapleton *et al.*, 2002) using the QuikChangeII site-directed mutagenesis kit (Stratagene) and the primers CS10 (GTCGCGCTCA***G***GCAGGAACGG) and CS11 (CCGTTCCTGC***C***TGAGCGCGAC). This step resulted in cloning intermediate 7 (*LD23835-bubR1*^{kd}) The *bubR1* or *bubR1*^{kd} sequences were amplified from *LD23835* or cloning intermediate 7, respectively, using the primers CS8 (TTGAG***GCGGCCGC***T**ATG**GACTTT**TGA**CAATGCGAA) and CS9 (CAAGA***CTCGAG***CTATTTCTGCAATATCGTGTTAA), which introduced a TGA stop-codon by a frameshift directly after the start codon of the *bubR1* sequence and a flanking NotI or XhoI site, respectively. After digestion with NotI and XhoI, the PCR fragment was inserted into the corresponding sites in *pUAST-EGFP-MCS* (Schittenhelm *et al.*, 2007) resulting in *pUAST-EGFP-STOP* constructs.

pUAST-EGFP-bubR1 and *pUAST-EGFP-bubR1*^{kd}
Constructs for ectopic expression of wild type or kinase dead BubR1 N-terminally tagged with EGFP by the UAS/GAL4 system. Both *pUAST-EGFP-STOP* constructs were digested with *Not*I, and a primer hybrid of CS22 (GGCCCGCCCTCGAGCAATCG) and CS23 (GGCCCGATTGCTCGAGGGCG) was ligated in order to reverse the frameshift causing the premature stop in the *pUAST-EGFP-STOP* constructs. This resulted in *pUAST-EGFP-bubR1* and *pUAST-EGFP-bubR1*^{kd}.

pUAST-Mps1
Constructs for ectopic expression of wild type or kinase-dead Mps1 by the UAS/GAL4 system.
pUAST-EGFP-Mps1 was digested with Acc65I and NotI, and the resulting fragment containing the *Mps1* sequence was transposed into the respective sites in *pUAST*, resulting in *pUAST-Mps1*.

pUAST-10myc-Mps1 and *pUAST-10myc-Mps1^{kd}*
Constructs for ectopic expression of wild type or kinase dead Mps1 N-terminally tagged with 10xmyc by the UAS/GAL4 system. *10myc* was amplified from *pCaSpeR4-10myc-Nuf2* (Schittenhelm *et al.*, 2007) using the primers AF56 (TCTGGATT***GCGGCCGC***ATGGGCGGCGCCCATG) and AF57 (ATATCGCC***GCGGCCGC***GCCTGGGTTTTCGAATGCC), which introduced flanking NotI sites. After digestion with NotI, the PCR fragment was transposed into the NotI site in *pUAST-Mps1* or *pUAST-Mps1^{kd}*, respectively, resulting in *pUAST-10myc-Mps1* and *pUAST-10myc-Mps1^{kd}*.

pUAST-EGFP-Cenp-C^{C}-Mps1 and *pUAST-EGFP-Cenp-C^{C}-Mps1^{kd}*
Constructs for ectopic expression of fusion proteins of wild type or kinase dead Mps1 with the C-terminal domain of *Cenp-C* N-terminally tagged with EGFP by the UAS/GAL4 system. *EGFP-Cenp-C^{C}* was amplified without stop codon of Cenp-C from *pUAST-EGFP-Cenp-C^{C}* (Heeger *et al.*, 2005) using the primers AF9 (GGGAATTGGGAATTCGTTAAC) and AF11 (CAAAGATCCT***GCGGCCGC***ACTGCGTATACACATCAGCA), which introduced a flanking NotI site. After digestion with BglII and NotI, the PCR fragment was transposed into the two corresponding sites in *pUAST* resulting in cloning intermediate 8 (*pUAST-EGFP-CenpC^{C}ΔTAG*). The *Mps1* sequence was amplified from *pCaSpeR4-EGFP-gMps1* (Fischer *et al.*, 2004) and the *Mps1^{kd}* sequence was amplified from *pCaSpeR4-EGFP-gMps1^{kd}* with AF12 (GAATAAATCG***GCGGCCGC***GATGACCACGCCTGTGCC) and AF13 (TT***GGTACC***TTAATTGCTGTTGGCGGTTC), which introduced a flanking NotI or Asp718 site, respectively. After digestion with NotI and Asp718, the PCR fragments were transposed into the corresponding sites in cloning intermediate 8 resulting in *pUAST-EGFP-Cenp-C^{C}-Mps1* and *pUAST-EGFP-Cenp-C^{C}-Mps1^{kd}*.

pUAST-EGFP-Mps1-Nuf2 and *pUAST-EGFP-Mps1^{kd}-Nuf2*
Construct for ectopic expression of fusion proteins of wild type or kinase dead Mps1 with Nuf2 N-terminally tagged with EGFP by the UAS/GAL4 system. The *Mps1* and *Mps1^{kd}* sequences were amplified from *pUAST-EGFP-Mps1* and *pUAST-EGFP-Mps1^{kd}* using the primers RaS27 (TCGTGACCGCCGCCGGG) and CS13 (GCTTT***GCGGCCGC***ATTGCTGTTGGCGGTTCTGC), which introduced a flanking NotI site. After digestion with NotI, the PCR fragments were transposed into the corresponding site in *pUAST-EGFP-Nuf2* (Schittenhelm *et al.*, 2007) resulting in *pUAST-EGFP-Mps1-Nuf2* and *pUAST-EGFP-Mps1^{kd}-Nuf2*.

pUAST-Torso(EC/TM)-EGFP-Mps1
Construct for ectopic expression of a fusion protein of Mps1 with the **e**xtra**c**ellular and **t**rans-**m**embrane domain (EC/TM) of Torso receptor tyrosine kinase internally tagged with EGFP by the UAS/GAL4 system. The *EGFP-Mps1* sequence was amplified from *pUAST-EGFP-Mps1* using the primers AF42 (CCTCCTGGGTCA***CCATGG***TGAGCAAGGGCGAGG) and AF43 (AGCTG***GCTAGC***TATCTTATAAGTAAACGCAAATTA), which introduced a flanking NheI or Eco91I site, respectively. After digestion with NheI and Eco91I, the PCR fragment was transposed into the corresponding sites in *pUAST-Torso-HA-CycA* (Dienemann and Sprenger, 2004) to replace the *HA-CycA* sequence resulting in *pUAST-Torso-EGFP-Mps1*.

pUAST-Torso(EC/TM)^{4021}-EGFP-Mps1
Construct for ectopic expression of a fusion protein of Mps1 with the **e**xtra**c**ellular and **t**rans-**m**embrane domain (EC/TM) of Torso receptor tyrosine kinase carrying a point mutation to allow receptor-independent dimerization internally tagged with EGFP by the UAS/GAL4 system. *pUAST-Torso(EC/TM)-EGFP-Mps1* was digested with NotI and the resulting

Torso(EC/TM)-EGFP fragment was inserted in the corresponding site in *pBluescriptII KS(-)* resulting in cloning intermediate 9: *pBluescript-Torso(EC/TM)-EGFP*. The point mutation A980G in the *Torso* coding sequence leading to the amino acid exchange Tyr327 to Cys (as in the gain-of-function allele $Torso^{4021}$ (Sprenger and Nusslein-Volhard, 1992)) was introduced into cloning intermediate 9 using the QuikChangeII site-directed mutagenesis kit (Stratagene) and the primers AF47 (CCGGATAACT***G***TACACTTCACATC) and AF48 (GTGAAGTGTA***C***AGTTATCCGGC). This step resulted in cloning intermediate 10: *pBluescript-Torso(EC/TM)*^{4021}*-EGFP*. Cloning intermediate 10 and *pUAST-Torso(EC/TM)-EGFP-Mps1* were digested with NotI and the resulting *Torso(EC/TM)*^{4021}*-EGFP* fragment from cloning intermediate 10 replaced the respective fragment in the *pUAST-Torso(EC/TM)-EGFP-Mps1* construct resulting in *pUAST-Torso(EC/TM)*^{4021}*-EGFP-Mps1*.

pUAST-Cenp-C^C*-bubR1*

Construct for ectopic expression of a fusion protein of BubR1 with the C-terminal domain of Cenp-C N-terminally tagged with EGFP by the UAS/GAL4 system. *pUAST-EGFP-Cenp-*C^C*-Mps1* was digested with EcoRI and NotI and the resulting EGFP-Cenp-C^C fragment was transposed into the corresponding sites in *pUAST* resulting in cloning intermediate 11 (*pUAST-EGFP-Cenp-*C^C*-MCS*). The *bubR1* sequence was amplified as described for *pUAST-EGFP-STOP*. After digestion with NotI and XhoI, the PCR fragment was inserted into the two corresponding sites in cloning intermediate 11 resulting in cloning intermediate 12 (*pUAST-EGFP-Cenp-*C^C*-STOP*). Cloning intermediate 12 was digested with NotI, and a primer hybrid of CS22 (GGCCCGCCCTCGAGCAATCG) and CS23 (GGCCCGATTGCTCGAGGGCG) was ligated in order to reverse the frameshift causing the premature stop in *pUAST-EGFP-Cenp-*C^C*-STOP*. This resulted in *pUAST-EGFP-Cenp-*C^C*-bubR1*.

pCaSpeR4-i2xtdTomato-Cenp-C

Construct for the expression of Cenp-C internally tagged with 2xtdTomato under control of its cis-regulatory region. The *tdTom* (*tandemTomato*) sequence was amplified twice from *pRSET-B-tdTom* first using the primers SN1 (GGG***GGTACC***TGGTGAGCAAGGGCGAGG) and SN3 (AGCCGC***GCTAGC***CTTGTACAGCTCGTCCATGC), which introduced a flanking Acc65I or NheI site, respectively, and second using the primers SN4 (ATTGGG***GCTAGC***GTGAGCAAGGGCGAGGAG) and SN5 (CGC***GGATCC***GGTACCACTTGTACAGCTCGTCCATG), which introduced a flanking NheI or BamHI site, respectively. After digestion of the first PCR product with Acc65I and NheI, the fragment was transposed into the corresponding sites in *pSLfa1180fa* (Horn and Wimmer, 2000) resulting in cloning intermediate 13 (*pSL-tdTom*). After digestion of the second PCR product with NheI and BamHI the fragment was transposed into the corresponding sites in cloning intermediate 13 resulting in cloning intermediate 14 (*pSL-2xtdTom*). The *2xtdTom* sequence was excised from cloning intermediate 14 with Acc65I, and the fragment was transposed into the BsiWI site in *pCaSpeR4-Cenp-C* (Heeger *et al.*, 2005) resulting in *pCaSpeR4-i2xtdTom-Cenp-C*.

Supplemental Tables

Table S1: Drosophila strains

Genotype (all in w* background)	**Abbreviation**	**Reference**
P{w$^+$, matα4tub-GAL4-VP16}V2H/CyO	*mat-GAL4*	(Hacker and Perrimon, 1998)
P{ry$^+$, 2xsev-Hs-GAL4}332.5, ry^{506}	*Hs-GAL4*	(Ruberte *et al.*, 1995)
P{ry$^+$, 2xsev-Hs-GAL4}332.1; ry^{506}	*sev-GAL4*	(Ruberte *et al.*, 1995)
P{GawB}Bx^{MS1096}	*Bx-GAL4*	(Capdevila and Guerrero, 1994)
P{w$^+$, His2Av-mRFP1} II.2	*His2Av-mRFP*	(Schuh *et al.*, 2007)
P{w$^+$,gcid-EGFP-cid} II.1	*Cid-EGFP*	(Schuh *et al.*, 2007)
P{w$^+$, mRFP-Cenp-C} III.1	*mRFP-Cenp-C*	(Schittenhelm *et al.*, 2007)
P{w$^+$, gi2xtdTomato-Cenp-C} II.3	*Tom-Cenp-C*	this study
P{PTT-GA}Jupiter^{G00147}	*Jupiter-GFP*	(Morin *et al.*, 2001)
P{w$^+$, UAS-EGFP-stop-BubR1} II.1	*UAS-EGFP*	this study
P{Ubi-GFP.nls} 3L1, P{Ubi-GFP.nls} 3L2, P{FRT(w^{hs})}2A	*Ubi-GFP*	(Luschnig *et al.*, 2004)
P{hsFLP}22, yw; P{neoFRT}82B, P{ovoD1-18}3R/TM3, Sb	*Hs-Flp; Ovo^{D1}/ TM3, Sb*	(Chou and Perrimon, 1996)
w; stg^{7B}, P{w$^+$, Hs-stg}/TM3, Sb, P{w$^+$, Ubx-lacZ}*	*stg^{7B}, Hs-stg/TM3*	(Sauer *et al.*, 1995)
rad21^{ex3}/TM3, Sb, P{w$^+$, Ubx-lacZ}	*rad21^{ex3}/TM3*	(Pauli *et al.*, 2008)
2xtub>rad21(271-3TEV)-myc	*rad21^{TEV}*	(Pauli *et al.*, 2008)
10UAS-nls-v5-TEV-nls2 II.83	*UAS-TEV*	(Pauli *et al.*, 2008)
dp, mad1^1/CyO	*mad1^1/CyO*	(Emre *et al.*, 2011)
Df(2R)w45-30n, cn^1/CyO	*Df(mad1)/CyO*	(Konev *et al.*, 1991)
P{w$^+$, mCherry-mad1}II	*Cherry-mad1*	(Emre *et al.*, 2011)
P{w$^+$, mad1-GFP}X	*mad1-GFP*	(Emre *et al.*, 2011)
P{EP}mad2^{G6595}	*mad2^P*	(Buffin *et al.*, 2007)
yw; bubR1^1, P{w$^+$, RFP-bubR1^{KEN}}	*bubR1^{KEN}*	(Rahmani *et al.*, 2009)
P{w$^+$, GFP-bubR1}X	*GFP-bubR1*	(Buffin *et al.*, 2005)
P{neoFRT}82B, ald^{B4}/TM3, Sb, P{w$^+$, Ubx-lacZ}	*Mps1^{aldB4}/TM3*	(Page *et al.*, 2007)
P{w$^+$, gEGFP-Mps1} *II.1* *II.2* *III.1* *III.4* recombinant *II.1, II.2*	*gEGFP-Mps1*	(Fischer *et al.*, 2004)
P{w$^+$, gEGFP-Mps1^{kd}} *II.3* *III.1*	*gEGFP-Mps1^{kd}*	this study
P{w$^+$, gEGFP-Mps1^N} *II.2* *III.1*	*gEGFP-Mps1^N*	this study
P{w$^+$, gEGFP-Mps1^C} *III.1* recombinant *II.3, II.4*	*gEGFP-Mps1^C*	this study
P{w$^+$, UAS-Mps1} II.4		this study

P{w$^+$, UAS-EGFP-Mps1} II.1 III.1	*E-Mps1*	this study
P{w$^+$, UAS-EGFP-Mps1^{kd}} III.1 recombinant *III.1, III.2*	*E-Mps1^{kd}*	this study
P{w$^+$, UAS-EGFP-Mps1^{N}} III.1	*E-Mps1^{N}*	this study
P{w$^+$, UAS-EGFP-Mps1^{C}} III.1	*E-Mps1^{C}*	this study
P{w$^+$, UAS-EGFP-Mps1^{C,kd}} III.1	*E-Mps1^{Ckd}*	this study
P{w$^+$, UAS-10myc-Mps1} II.6	*myc-Mps1*	this study
P{w$^+$, UAS-10myc-Mps1^{kd}} III.1	*myc-Mps1^{kd}*	this study
P{w$^+$, UAS-EGFP-Cenp-C^{C}-Mps1} II.1	*EC-Mps1*	this study
P{w$^+$, UAS-EGFP-Cenp-C^{C}-Mps1^{kd}} II.1	*EC-Mps1^{kd}*	this study
P{w$^+$, UAS-EGFP-Mps1-Nuf2} II.1		this study
P{w$^+$, UAS-EGFP-Mps1^{kd}-Nuf2} II.1		this study
P{w$^+$, UAS-Torso(EC/TM)-EGFP-Mps1} II.1, II.2/CyO; III.1, III.2, III.7		this study
P{w$^+$, UAS-Torso(EC/TM)^{4021}-EGFP-Mps1} II.1		this study
P{w$^+$, UAS-EGFP-bub1} II.1 III.1	*E-bub1*	this study
P{w$^+$, UAS-EGFP-bubR1} II.1 III.1	*E-bubR1*	this study
P{w$^+$, UAS-EGFP-bubR1^{kd}} II.1 III.1	*E-bubR1^{kd}*	this study
P{w$^+$, UAS-EGFP-Cenp-C^{C}-bubR1} II.1 III.1	*EC-bubR1*	this study
P{w$^+$, UAS-EGFP-mad2} II.1 III.1	*E-mad2*	this study

Supplemental Table S2: Genotype of displayed data

Figure	Genotype	Comments
Figure 1		
A	*gEGFP-Mps1 II.1, II.2; mRFP-Cenp-C*	
B		
wt	*gEGFP-Mps1 II.1, II.2*	
N	*gEGFP-Mps1^{N} II.2*	
C	*gEGFP-Mps1^{C} II.3, II.4*	
kd	*gEGFP-Mps1^{kd} II.3*	
C		Extracts from larvae with one copy of *Hs-GAL4* and one copy of each of the listed *UAS* transgenes.
wt/wt	*UAS-myc-Mps1 II.6; UAS-EGFP-Mps1 III.1*	
kd/wt	*UAS-myc-Mps1^{kd} II.6; UAS-EGFP-Mps1 III.1*	
wt/kd	*UAS-myc-Mps1^{kd} III.1, UAS-EGFP-Mps1 III.1*	
kd/kd	*UAS-myc-Mps1^{kd} III.1, UAS-EGFP-Mps1^{kd} III.1*	
-/kd	*UAS-EGFP II.1; UAS-myc-Mps1^{kd} III.1*	
D		Embryos derived from mothers with germline clones of the listed genotypes.
wt	*Hs-Flp/+; gEGFP-Mps1 II.1, II.2/+; Mps1^{aldB4}*	
N	*Hs-Flp/+; gEGFP-Mps1^{N} II.2/+; Mps1^{aldB4}*	
C	*Hs-Flp/+; gEGFP-Mps1^{C} II.3, II.4/+; Mps1^{aldB4}*	
kd	*Hs-Flp/+; gEGFP-Mps1^{kd} II.3/+; Mps1^{aldB4}*	
Figure 2		
A		
Mad1-GFP	*mad1-GFP*	
GFP	*Ubi-GFP*	
B		
wt	*Cherry-mad1; gEGFP-Mps1 III.1*	
kd	*Cherry-mad1; gEGFP-Mps1^{kd} III.1*	
N	*Cherry-mad1; gEGFP-Mps1^{N} III.1*	
C	*Cherry-mad1; gEGFP-Mps1^{C} III.1*	
-	*Cherry-mad1; Ubi-GFP*	
C		Embryos derived from mothers with the listed genotype. Additional genotypes analyzed for the bar diagram: - *gEGFP-Mps1 III.4* - *gEGFP-Mps1 II.1, II.2* - *mad1^{1} Df(mad1); gEGFP-Mps1 III.4*.
wt	*gEGFP-Mps1 III.1*	
mad1^{-}	*mad1^{1}/Df(mad1); gEGFP-Mps1 III.1*	
mad2^{-}	*gEGFP-Mps1 II.1, II.2; mad2^{P}*	
D		Embryos derived from mothers with the listed genotype, in case of *Mps1^{-}* only in germline clones.
wt	*mad1-GFP*	
Mps1^{-}	*mad1-GFP; Mps1^{aldB4}*	
mad2^{-}	*mad1-GFP; mad2^{P}*	

Figure 3

A	*stg^{7B}, Hs-stg*	
B	*w^{1}*	
C		Extracts from embryos derived from mothers with germline clones of the listed genotypes.
wt	*Hs-Flp/+; gEGFP-Mps1 II.1, II.2/+; Mps1^{aldB4}*	
kd	*Hs-Flp/+; gEGFP-Mps1^{kd} II.3/+; Mps1^{aldB4}*	
N	*Hs-Flp/+; gEGFP-Mps1^{N} II.2/+; Mps1^{aldB4}*	
D	*W^{1}*	

Figure 4

A	*(no UAS transgene)*	Embryos derived from *mat-GAL4* mothers with one copy of the listed *UAS* transgenes inherited from the father.
A,B	*UAS-EGFP-Cenp-C^{C}-Mps1^{kd} II.1*	
A,B	*UAS-EGFP-Cenp-C^{C}-Mps1 II.1*	
A	*UAS-EGFP-Mps1 II.1*	
A	*UAS-EGFP-Mps1^{kd} III.1, III.2*	
C		
wt	*w^{1}*	
E-Mps1	*UAS-EGFP-Mps1 II.1*	as above
D		
E-Mps1	*UAS-EGFP-Mps1 II.1*	as above
EC-Mps1	*UAS-EGFP-Cenp-C^{C}-Mps1 II.1.*	as above

Figure 5

A		Embryos derived from *mat-GAL4, His2Av-mRFP, Cid-EGFP/CyO* mothers and one copy of the listed *UAS* transgenes inherited from the father.
wt	*w^{1}*	
Mps1 OE	*UAS-Mps1 II.4*	
B-G		Embryos derived from the indicated crosses with mothers providing maternally derived Gal4. *Mps1* OE, *mad2^{P}*: PCR genotyping after in vivo imaging for identification of *UAS* transgene.
wt	*mat-GAL4, Tom-Cenp-C/CyO; Jupiter-GFP* x *w^{1}*	
Mps1 OE	*mat-GAL4, Tom-Cenp-C/CyO; Jupiter-GFP* x *UAS-Mps1 II.4*	
mad2^{P}	*mat-GAL4, Tom-Cenp-C/CyO; Jupiter-GFP, mad2^{P}* x *mad2^{P}*	
Mps1 OE *mad2^{P}*	*mat-GAL4, Tom-Cenp-C/CyO; Jupiter-GFP, mad2^{P}* x *UAS-Mps1 II.4/CyO, mad2^{P}*	

Figure 6

A-C		Embryos derived from the indicated crosses with mothers providing maternally derived Gal4.
wt	*GFP-bubR1/+; mat-GAL4, His2Av-mRFP/+* x *w^{1}*	
Mps1 OE	*GFP-bubR1/+; mat-GAL4, His2Av-mRFP/+* x *UAS-Mps1 II.4*	
D		Embryos derived from the indicated crosses with mothers providing maternally derived Gal4.
wt	*GFP-bubR1/+; mat-GAL4, His2Av-mRFP/+; mad2^{P} x mad2^{P}*	
Mps1 OE	*GFP-bubR1/+; mat-GAL4, His2Av-mRFP/+; mad2^{P}* x *UAS-Mps1 II.4/CyO; mad2^{P}*	

Figure 7

A		Embryos derived from the indicated crosses with mothers providing Gal4. PCR genotyping after in vivo imaging for identification of *rad21^{ex3}*, *mad2^{P}* and *UAS* transgenes.
–TEV	*2xrad21^{TEV}/mat-GAL4, His2Av-mRFP, Cid-EGFP; rad21^{ex3}, mad2^{P}* x *UAS-TEV, UAS-Mps1 II.4; rad21^{ex3}, mad2^{P}/TM6*	
+TEV	*2xrad21^{TEV}/mat-GAL4, His2Av-mRFP, Cid-EGFP; rad21^{ex3}, mad2^{P}* x *UAS-Mps1 II.4; rad21^{ex3}, mad2^{P}/TM6*	
B		Embryos derived from the indicated crosses with mothers providing Gal4. PCR genotyping after in vivo imaging for identification of *rad21^{ex3}*, *mad2^{P}* and *UAS* transgenes.
–TEV	see above	
+TEV	see above	
–TEV/-Mps1	*mat-GAL4, His2Av-mRFP, Cid-EGFP/CyO; mad2^{P} x mad2^{P}*	
+TEV/+Mps1	*mat-GAL4, His2Av-mRFP, Cid-EGFP/+; rad21^{ex3}, mad2^{P}/mad2^{P}* x *UAS-TEV, UAS-Mps1 II.4/CyO ; rad21^{ex3}, mad2^{P}/TM6*	

Supplemental Figure 2

A		
wt	*Hs-GAL4/+*	
UAS-E-Mps1	*Hs-GAL4/UAS-EGFP-Mps1 III.1*	
B		Extracts from syncytial embryos derived from mothers with germline clones of the listed genotypes. No germline clones in case of *w^{1}*.
wt	*Hs-Flp/+; gEGFP-Mps1 II.1, II.2/+; Mps1^{aldB4}*	
kd	*Hs-Flp +; gEGFP-Mps1^{kd} II.3/+; Mps1^{aldB4}*	
N	*Hs-Flp/+; gEGFP-Mps1^{N} II.2/+ ; Mps1^{aldB4}*	
C	*Hs-Flp/+; gEGFP-Mps1^{C} II.3, II.4/+;Mps1^{aldB4}*	
-	*Hs-Flp/+; Mps1^{aldB4}*	
Mps1^{+}	*w^{1}*	

Supplemental Figure 3

A	*UAS-EGFP-Mps1 II.1*	Embryos derived from *mat-GAL4* mothers with one copy of the listed *UAS* transgenes inherited from the father.
B	*UAS-EGFP-Mps1 III.1*	
C	*UAS-EGFP-Mps1^{kd} III.1, III.2*	
D		
II.1	*UAS-EGFP-Mps1 II.1*	
III.1	*UAS-EGFP-Mps1 III.1*	
kd III.1, III.2	*UAS-EGFP-Mps1^{kd} III.1, III.2*	

Supplemental Figure 4

A	*gEGFP-Mps1 II.1/CyO; Mps1^{aldB4}* x *gEGFP-Mps1 II.1; Mps1^{aldB4}*	Embryos derived from the indicated crosses with mothers providing Gal4. B: For comparison of fluorescence intensities *gEGFP-Mps II.2; Mps1^{aldB4}* was used as reference as in A.
B	*mat-GAL4, gEGFP-Mps1 II.2/CyO; Mps1^{aldB4}* x *UAS-EGFP-Cenp-C^{C}-Mps1 II.1, gEGFP-Mps1 II.2; Mps1^{aldB4}*	
C	*mat-GAL4, gEGFP-Mps1 II.1/CyO; Mps1^{aldB4}* x *UAS-EGFP-Mps1 II.1, gEGFP-Mps1 II.1; Mps1^{aldB4}*	

Supplemental references

Buffin, E., Emre, D., and Karess, R.E. (2007). Flies without a spindle checkpoint. Nat Cell Biol *9*, 565-572.

Buffin, E., Lefebvre, C., Huang, J., Gagou, M.E., and Karess, R.E. (2005). Recruitment of Mad2 to the kinetochore requires the Rod/Zw10 complex. Curr Biol *15*, 856-861.

Chou, T.B., and Perrimon, N. (1996). The autosomal FLP-DFS technique for generating germline mosaics in Drosophila melanogaster. Genetics *144*, 1673-1679.

Dienemann, A., and Sprenger, F. (2004). Requirements of cyclin a for mitosis are independent of its subcellular localization. Curr Biol *14*, 1117-1123.

Emre, D., Terracol, R., Poncet, A., Rahmani, Z., and Karess, R.E. (2011). A mitotic role for Mad1 beyond the spindle checkpoint. J Cell Sci *124*, 1664-1671.

Fischer, M.G., Heeger, S., Hacker, U., and Lehner, C.F. (2004). The mitotic arrest in response to hypoxia and of polar bodies during early embryogenesis requires Drosophila Mps1. Curr Biol *14*, 2019-2024.

Foe, V.E. (1989). Mitotic domains reveal early commitment of cells in Drosophila embryos. Development *107*, 1-22.

Hacker, U., and Perrimon, N. (1998). DRhoGEF2 encodes a member of the Dbl family of oncogenes and controls cell shape changes during gastrulation in Drosophila. Genes Dev *12*, 274-284.

Heeger, S., Leismann, O., Schittenhelm, R., Schraidt, O., Heidmann, S., and Lehner , C.F. (2005). Genetic inteactions of Separase regulatory subunits reveal the diverged Drosophila Cenp-C homolog. Genes Dev *19*, 2041-2053.

Horn, C., and Wimmer, E.A. (2000). A versatile vector set for animal transgenesis. Dev. Genes Evol. *210*, 630-637.

Konev, A., Varentsova, E.R., Sarantseva, S.V., and Khromykh Iu, M. (1991). [Cytogenetic analysis of chromosome segments containing radiosensitivity genes in Drosophila. Radiation mutagenesis in the 44-45 region of chromosome 2 of Drosophila melanogaster]. Genetika *27*, 77-87.

Luschnig, S., Moussian, B., Krauss, J., Desjeux, I., Perkovic, J., and Nusslein-Volhard, C. (2004). An F1 genetic screen for maternal-effect mutations affecting embryonic pattern formation in Drosophila melanogaster. Genetics *167*, 325-342.

Morin, X., Daneman, R., Zavortink, M., and Chia, W. (2001). A protein trap strategy to detect GFP-tagged proteins expressed from their endogenous loci in Drosophila. Proc Natl Acad Sci U S A *98*, 15050-15055.

Page, S.L., Nielsen, R.J., Teeter, K., Lake, C.M., Ong, S., Wright, K.R., Dean, K.L., Agne, D., Gilliland, W.D., and Hawley, R.S. (2007). A germline clone screen for meiotic mutants in Drosophila melanogaster. Fly (Austin) *1*, 172-181.

Pauli, A., Althoff, F., Oliveira, R.A., Heidmann, S., Schuldiner, O., Lehner, C.F., Dickson, B.J., and Nasmyth, K. (2008). Cell-type-specific TEV protease cleavage reveals cohesin functions in Drosophila neurons. Dev Cell *14*, 239-251.

Rahmani, Z., Gagou, M.E., Lefebvre, C., Emre, D., and Karess, R.E. (2009). Separating the spindle, checkpoint, and timer functions of BubR1. J Cell Biol *187*, 597-605.

Ruberte, E., Marty, T., Nellen, D., Affolter, M., and Basler, K. (1995). An absolute requirement for both the type II and type I receptors, punt and thick veins, for dpp signaling in vivo. Cell *80*, 889-897.

Rubin, G.M., Yandell, M.D., Wortman, J.R., Gabor Miklos, G.L., Nelson, C.R., Hariharan, I.K., Fortini, M.E., Li, P.W., Apweiler, R., Fleischmann, W., Cherry, J.M., Henikoff, S., Skupski, M.P., Misra, S., Ashburner, M., Birney, E., Boguski, M.S., Brody, T., Brokstein, P., Celniker, S.E., Chervitz, S.A., Coates, D., Cravchik, A., Gabrielian, A., Galle, R.F., Gelbart, W.M., George, R.A., Goldstein, L.S., Gong, F., Guan, P., Harris, N.L., Hay, B.A.,

Hoskins, R.A., Li, J., Li, Z., Hynes, R.O., Jones, S.J., Kuehl, P.M., Lemaitre, B., Littleton, J.T., Morrison, D.K., Mungall, C., O'Farrell, P.H., Pickeral, O.K., Shue, C., Vosshall, L.B., Zhang, J., Zhao, Q., Zheng, X.H., and Lewis, S. (2000). Comparative genomics of the eukaryotes. Science *287*, 2204-2215.

Sauer, K., Knoblich, J.A., Richardson, H., and Lehner, C.F. (1995). Distinct modes of cyclin E/cdc2c kinase regulation and S phase control in mitotic and endoreduplication cycles of Drosophila embryogenesis. Genes Dev. *9*, 1327-1339.

Schittenhelm, R.B., Heeger, S., Althoff, F., Walter, A., Heidmann, S., Mechtler, K., and Lehner, C.F. (2007). Spatial organization of a ubiquitous eukaryotic kinetochore protein network in Drosophila chromosomes. Chromosoma *116*, 385-402.

Schuh, M., Lehner, C.F., and Heidmann, S. (2007). Incorporation of Drosophila CID/CENP-A and CENP-C into centromeres during early embryonic anaphase. Curr Biol *17*, 237-243.

Sprenger, F., and Nusslein-Volhard, C. (1992). Torso receptor activity is regulated by a diffusible ligand produced at the extracellular terminal regions of the Drosophila egg. Cell *71*, 987-1001.

Stapleton, M., Carlson, J., Brokstein, P., Yu, C., Champe, M., George, R., Guarin, H., Kronmiller, B., Pacleb, J., Park, S., Wan, K., Rubin, G.M., and Celniker, S.E. (2002). A Drosophila full-length cDNA resource. Genome Biol *3*, RESEARCH0080.0081-0080.0088.

Supplemental Figure 1

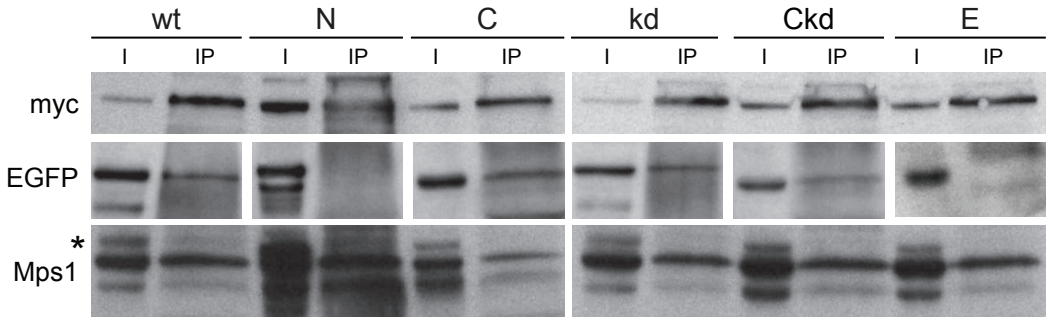

Supplemental Figure 1. Mps1-Mps1 interaction. Extracts from S2R+ cells were prepared after transient transfection with *pCaSpeR4-Act5C-GAL4*, *pUAST-myc-Mps1* and an additional *pUAST* construct encoding EGFP fused to either wild-type Mps1 (wt), N-terminal regulatory domain (N), C-terminal kinase domain (C), kinase-dead Mps1 (kd), kinase-dead C-terminal kinase domain (Ckd) or nothing (E). Immunoprecipitation was performed with anti-myc. Extracts (I) and immunoprecipitates (IP) were analyzed by immunoblotting. Immunoblotting with anti-myc (myc) revealed the presence of similar levels of myc-Mps1 in all of the immunoprecipitates. Immunoblotting with anti-EGFP (EGFP) revealed co-immunoprecipitation of myc-Mps1 and EGFP-Mps1 (wt), EGFP-Mps1^{kd} (kd), EGFP-Mps1^{C} (C), EGFP-Mps1^{Ckd} (Ckd) but not EGFP-Mps1^{N} (N) and EGFP (E). Only the regions with these different EGFP versions are displayed. Immunoblotting with anti-Mps1 (Mps1) revealed co-immunoprecipitation of myc-Mps1 and endogenous Mps1. Anti-Mps1 also reacted with EGFP-Mps1 fusion proteins but for clarity only the region with endogenous Mps1 is displayed. A cross-reaction of anti-Mps1 present in the extract lanes is marked with an asterisk. The immunoprecipitate loaded in the IP lanes was isolated from 60-fold more extract than that loaded in the I lanes.

Supplemental Figure 2

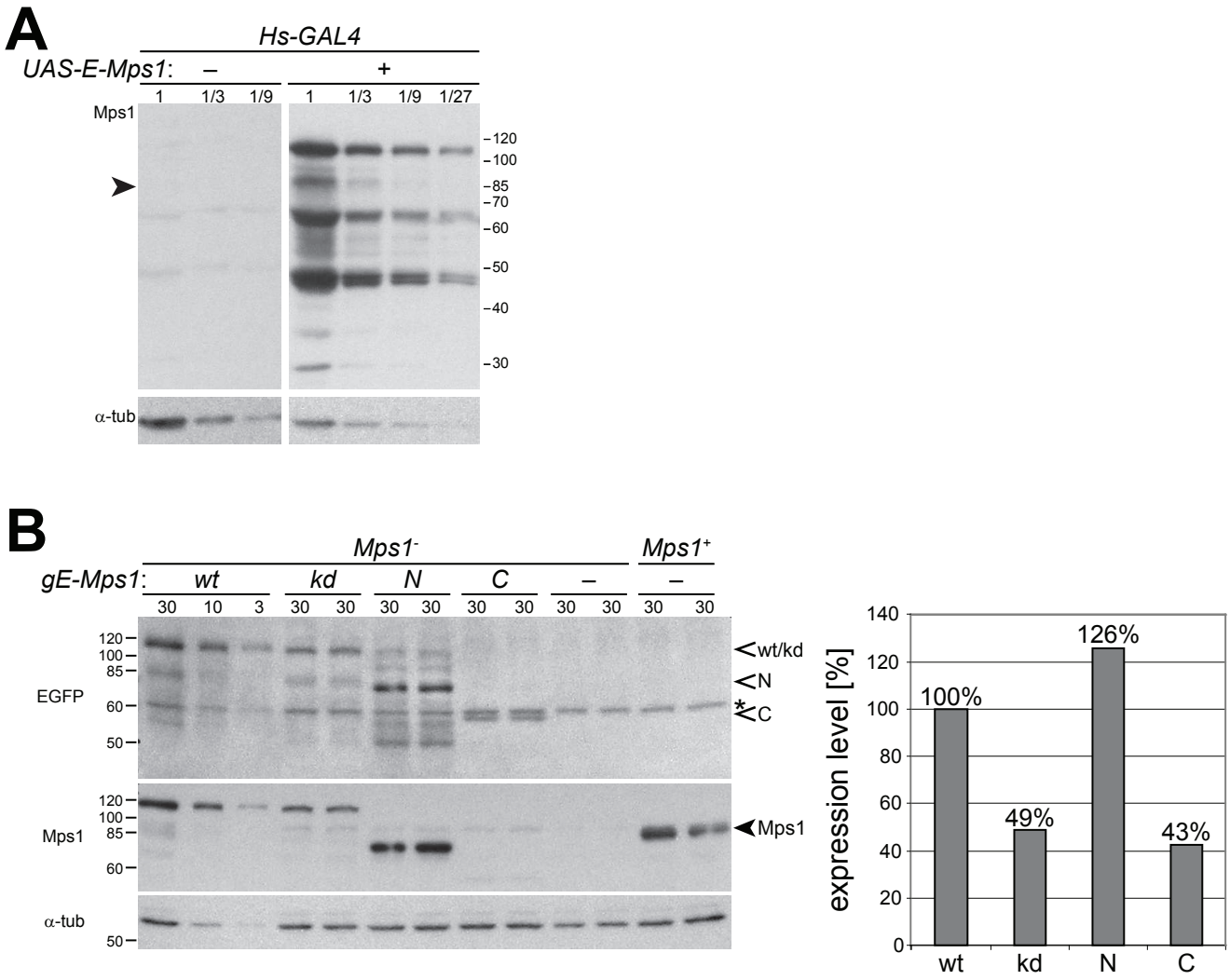

Supplemental Figure 2. Levels of Mps1 expressed from transgenes and endogenous locus. (A) Extracts from third instar wandering stage *Hs-GAL4* larvae without (*wt*) or with a *UAS-EGFP-Mps1* transgene (*UAS-E-Mps1*) were prepared after 2 hours of incubation at 37°C and 1 hour of recovery at 25°C. Serial dilutions were loaded as indicated by the numbers above the lanes which indicate larva equivalents. Immunoblotting with anti-α-tubulin (α-tub) served as loading control. Immunoblotting with anti-Mps1 (Mps1) indicated that the resulting expression level of EGFP-Mps1 is at least 30-fold higher than that of endogenous Mps1. The position of wild-type Mps1 is indicated by an arrowhead. The position of molecular weight markers is indicated on the right side. (B) Extracts were prepared from syncytial embryos derived from females with $Mps1^{aldB4}$ germline clones ($Mps1^{-}$) or from $Mps1^{+}$ females ($Mps1^{+}$). Transgenes under control of the *Mps1* cis-regulatory region driving expression of EGFP fused to either wild-type Mps1 (*wt*), kinase-dead Mps1 (*kd*), N-terminal region of Mps1 (*N*), or C-terminal region of Mps1 (*C*) were present in these females as indicated. The serial dilution in the three lanes on the left was used for comparison of expression levels detected by immunoblotting in the other duplicate lanes. The numbers above each lane indicate the embryo equivalents loaded. Immunoblotting with anti-α-tubulin (α-tub) served as loading control. Immunoblotting with anti-EGFP (EGFP) and anti-Mps1 (Mps1) was used to detect expression of transgene products and endogenous Mps1. The position of the transgene products is indicated by open arrowheads and the position of endogenous Mps1 with a filled arrowhead. A cross-reaction of anti-EGFP is marked with an asterisk. The position of molecular weight markers is indicated on the left side. The results from quantification of the expression levels of the transgene products are shown in the bar diagram.

Supplemental Figure 3

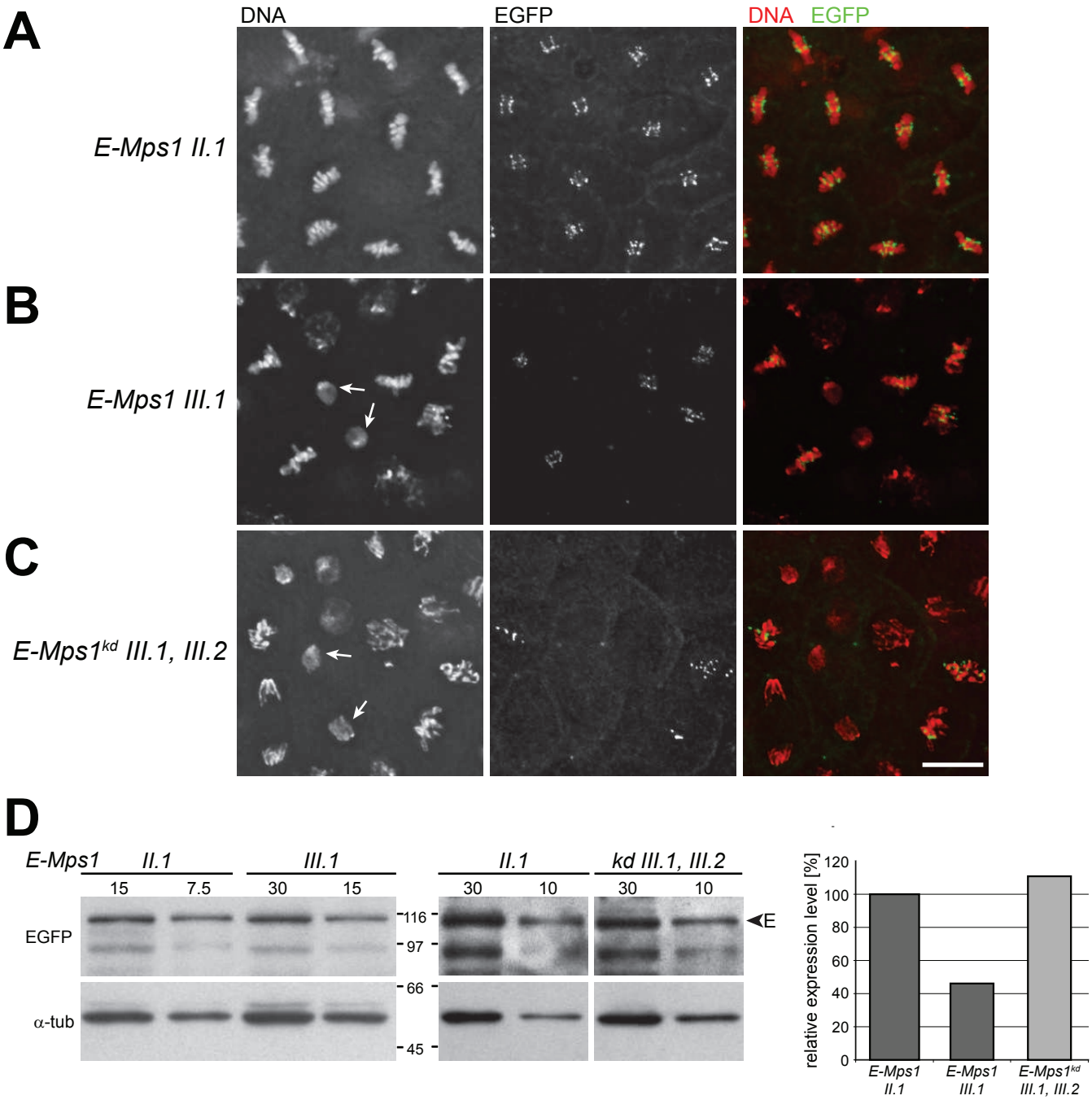

Supplemental Figure 3. Induction of metaphase delay by excess Mps1 depends on expression level and kinase activity. (A–C) The UAS/GAL4 system was used for expression of EGFP-Mps1 or EGFP-Mps1^{kd} from different *UAS* transgene insertions before mitosis 14. Embryos were fixed at the stage of mitosis 14. The epidermal regions with mitotic domain 10 (Foe, 1989) are displayed after DNA labelling. (A) *UAS-EGFP-Mps1 II.1* (*E-Mps1 II.1*) results in a relatively high level expression (see D) and an extended metaphase delay, as revealed by the drastic enrichment of metaphase plates. (B) *UAS-EGFP-Mps1 III.1* (*E-Mps1 III.1*) results in a relatively low level of expression (see D) that does not cause a metaphase delay during mitosis 14. No enrichment of metaphase plates was observed. (C) The combination of *UAS-EGFP-Mps1^{kd} III.1* and *III.2* (*E-Mps1^{kd} III.1, III.2*) results in an expression level that is slightly higher than *UAS-EGFP-Mps1 II.1* (see D) but the kinase-dead transgene product does not cause a metaphase delay. No enrichment of metaphase plates was observed. Bar corresponds to 10 μm. (D) Expression levels obtained with the transgenes and at the same stage as analyzed in A–C were determined by quantitative immunoblotting with antibodies against EGFP (EGFP) and α-tubulin (α-tub) which was used as a loading control. Serial dilutions of embryo extracts were loaded with numbers on top of the lanes representing embryo equivalents. The position of EGFP-Mps1 and EGFP-Mps1^{kd} is indicated by an arrowhead. The position of molecular weight markers is indicated between the panels. The two panels on the right side represent regions from the same immunoblot. The results from quantification of the expression levels of the transgene products are shown in the bar diagram.

Supplemental Figure 4

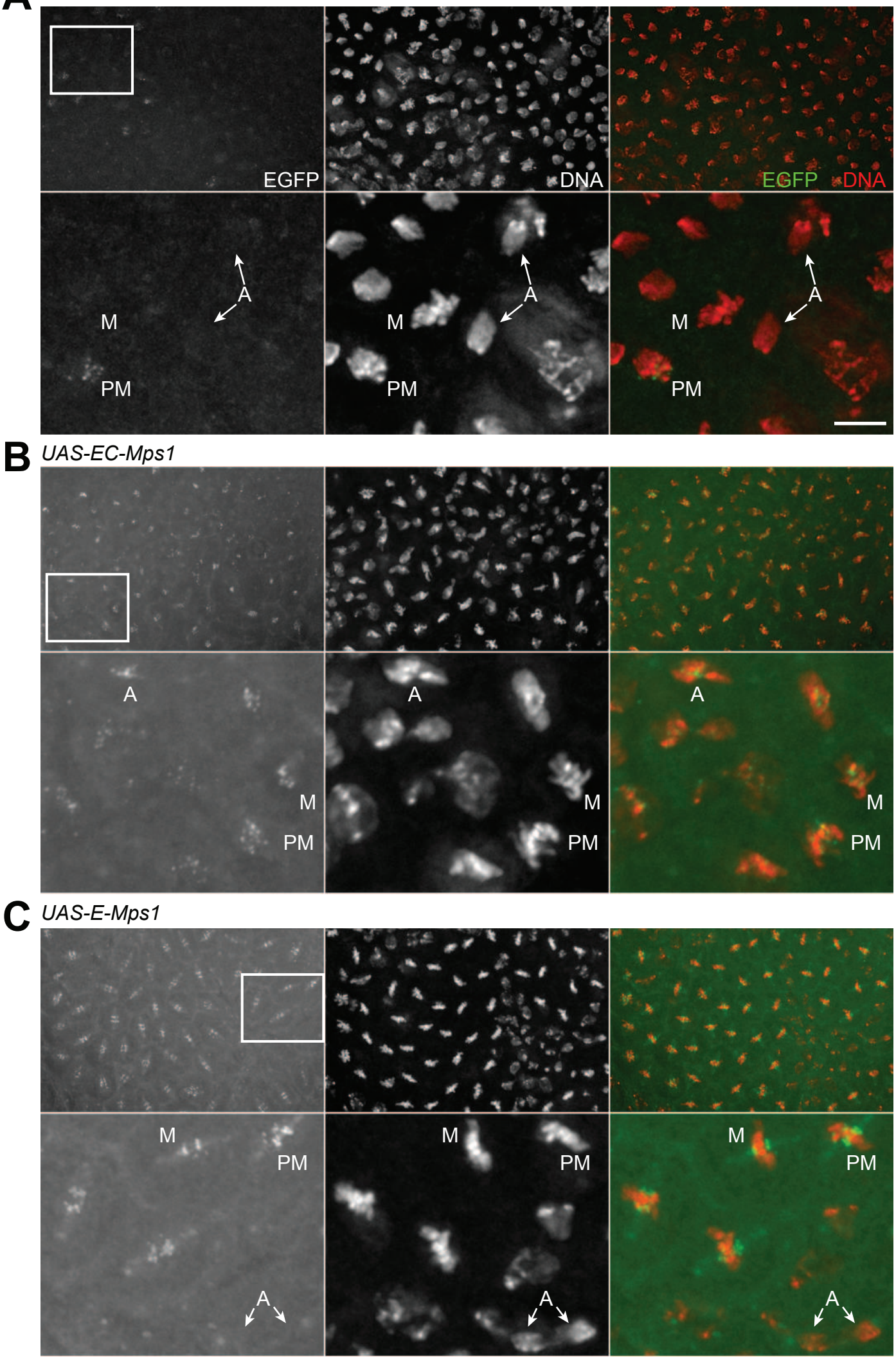

Supplemental Figure 4. Comparison of kinetochore levels of EGFP-Mps1 variants. (A–C) The UAS/GAL4 system was either not used (A, no *UAS*) or used for expression of *EGFP-CenpC^{C}-Mps1* (B, *EC-Mps1*) or EGFP-Mps1 (C, *E-Mps1*) before mitosis 14 in *gEGFP-Mps1, Mps1^{aldB4}* embryos (A–C) which express no endogenous Mps1 because of the *Mps1^{aldB4}* mutation but EGFP-Mps1 from the *gEGFP-Mps1* transgene under control of the *Mps1* cis-regulatory region. Embryos were fixed at the stage of mitosis 14. The epidermal regions with mitotic domain 10 (Foe, 1989) are displayed after DNA labelling. Bar in A corresponds to 5 µm. White frames indicate the regions shown at higher magnification in the rows below. Cells in prometaphase (PM), metaphase (M) and anaphase (A) are indicated in the high magnifications views. (A) After *EGFP-Mps1* expression at normal levels progression through mitosis 14 is normal and transient EGFP signals on kinetochores during prometaphase are comparatively weak. (B) When in addition *EGFP-CenpC^{C}-Mps1* is expressed as well, EGFP signals on kinetochores remain detectable throughout mitosis during which sister chromatids fail to be segregated to the poles, resulting in DNA bridges in ana- and telophase. (C) When *EGFP-Mps1* is overexpressed, EGFP signals on kinetochores are far stronger and remain detectable throughout the resulting metaphase delay. However, kinetochore signals are no longer observed during the eventual exit from mitosis. See main text for the results of EGFP signal quantifications.

Supplemental Figure 5

UAS-Transgene	Schematic Drawing	Mitosis 14	EGFP signal
E-Bub1		normal	NE remnants
E-BubR1		normal	kt until metaphase
E-BubR1^{kd}		normal	kt until metaphase
EC-BubR1		normal	kt persistent
EC-BubR1^{kd}		normal	kt persistent
E-Mad2		normal	kt until metaphase

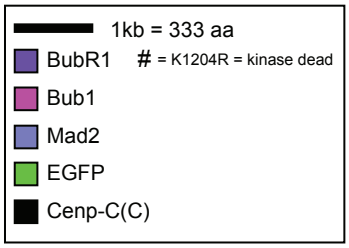

Supplemental Figure 5. Summary of *UAS* transgenes allowing expression of Drosophila SAC components other than Mps1. Schematic drawings illustrate the structure of the different variants. The effects on progression through mitosis 14 in mitotic domain 10 after expression of paternally derived *UAS* transgenes by maternally derived Gal4 are summarized, as well as the localization of the EGFP fusion proteins during mitosis. kt: kinetochore. NE remnants: remnants of the nuclear envelope.

Supplemental Figure 6

UAS transgene	structure	expression in embryonic cycle 14			expression in imaginal discs	
		level	progression through mitosis	kinetochore signals	eye	wing
Mps1		*II.4*: 10x	metaphase delay		nd	nd
E-Mps1		*II.1*: 5x	metaphase delay	kt until M/A	smaller, rough	nd
		III.1: 2.5x	normal	kt until M/A	slightly rough	tiny or absent
E-Mps1^{kd}		*III.1,III.2*: 5x	normal	kt until metaphase	nd	only partially unfolded
E-Mps1^{N}		*III.1*: 5x	normal	nd	wt	wt
E-Mps1^{C}		*III.1*: 2.5x	normal	nd	rough	not unfolded
E-Mps1^{C,kd}		*III.1*: 5x	normal	nd	nd	nd
EC-Mps1		*II.1*: 0.5x	cut	kt persistent	nd	nd
EC-Mps1^{kd}		*II.1*: 0.5x	normal	kt persistent	nd	nd
E-Mps1-Nuf2		*II.1*: 2.5x	normal	kt persistent	nd	nd
E-Mps1^{kd}-Nuf2		nd	normal	kt persistent	nd	nd
Tor-E-Mps1		*II.1, II.2, II.7; III.1, III.2*: 1.5x	weak metaphase delay, cut	(cell membrane)	nd	nd
Tor^{4021}-E-Mps1		*II.1*: 1x	wt	(cell membrane)	nd	nd

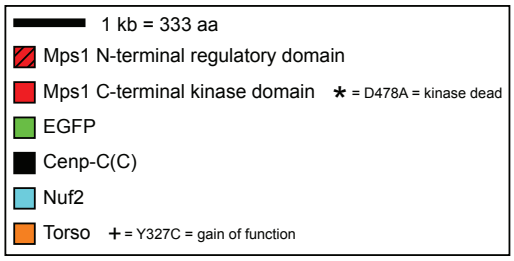

Supplemental Figure 6. Summary of *UAS* transgenes allowing expression of Mps1 variants. Schematic drawings illustrate the structure of the different Mps1 variants. The expression levels resulting during the stage of mitosis 14 when maternally derived Gal4 drives expression from paternally derived *UAS* transgenes were analyzed as described in Materials and methods (see also Figure 4, F and G and Supplemental Figure 3D), and are given relative to that of endogenous Mps1. The effects on progression through mitosis 14 in mitotic domain 10 are summarized, as well as the localization of the EGFP fusion proteins during mitosis. Moreover, the phenotypes of adult eyes and wings after expression of the EGFP fusion proteins in eye imaginal discs (by *sev* promoter driven *GAL4*) and in the wing imaginal discs (by *Bx* promoter driven *GAL4*) are described. kt: kinetochore. nd: not done

Supplemental Figure 7

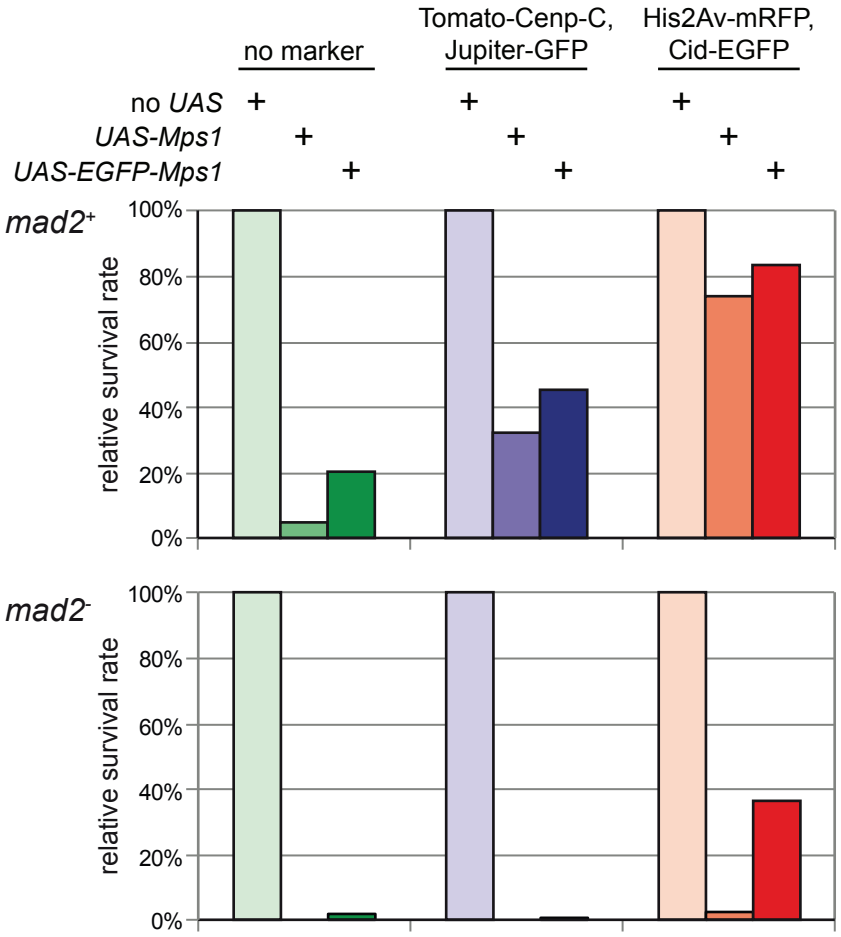

Supplemental Figure 7. Effects of various genetic backgrounds on successful development after transient *Mps1* overexpression. Females providing a maternal contribution of Gal4 as well as different fluorescent marker proteins (as indicated above the bars and by colors) were crossed with males carrying different *UAS* transgenes (as indicated above the bars and by color gradation) balanced over *CyO*. Progeny inheriting a *UAS* transgene from the father will express these transgenes transiently during the embryonic cell division cycles 14 – 16 because of the maternally provided Gal4. In contrast, there is no *UAS* transgene expression in the class of progeny inheriting the balancer chromosome from the father. Adult progeny with and without balancer chromosome was counted (n > 150). The bars indicate the fraction of adult progeny with the *UAS* transgene in percent of those without. The upper and lower panels describe the results obtained with *mad2*$^{+}$ and *mad2*$^{-}$ backgrounds, respectively. Interestingly, both combinations of fluorescent marker proteins protected partially from the lethal effects of excess Mps1 compared to the marker-free crosses, but only in the *mad2*$^{+}$ background. These findings are consistent with the assumption that the fluorescent marker combinations result in subtle problems during entry into mitosis which enhance the SAC activation by excess Mps1 and that the success of faithful chromosome segregation during anaphase after SAC adaptation might be improved by the increased cohesion fatigue during the resulting longer metaphase delay.